

1 **Title:** Elephant megacarcasses increase local nutrient pools in African savanna soils and plants

2

3 Courtney G. Reed^{1*}, Michelle L. Budny², Johan T. du Toit^{3,4}, Ryan Helcoski³, Joshua P.

4 Schimel¹, Izak P. J. Smit^{5,6}, Tercia Strydom⁵, Aimee Tallian^{3,7}, Dave I. Thompson^{8,9}, Helga van

5 Coller^{8,10}, Nathan P. Lemoine^{2,11}, Deron E. Burkepile^{1,8*}

6

7 ¹Department of Ecology, Evolution, and Marine Biology, University of California, Santa

8 Barbara, CA, USA

9 ²Department of Biological Sciences, Marquette University, Milwaukee, WI, USA

10 ³Department of Wildland Resources, Utah State University, Logan, UT, USA

11 ⁴Institute of Zoology, Zoological Society of London, London, England, UK

12 ⁵Scientific Services, South African National Parks, Skukuza, South Africa

13 ⁶Sustainability Research Unit, Nelson Mandela University, George, South Africa

14 ⁷Norwegian Institute for Nature Research, Høgskoleringen 9 Trondheim, 7485 Norway

15 ⁸South African Environmental Observation Network (SAEON), Ndlovu Node, Phalaborwa,

16 South Africa

17 ⁹Unit for Environmental Sciences and Management, Potchefstroom Campus, North West

18 University, Potchefstroom, South Africa

19 ¹⁰The Expanded Freshwater and Terrestrial Environmental Observation Network (EFTEON),

20 Kimberley 8306, South Africa

21 ¹¹Department of Zoology, Milwaukee Public Museum, Milwaukee, WI, USA

22

23 *Corresponding authors: Courtney Reed, courtneyreed@ucsb.edu, Deron Burkepile,
24 dburkepile@ucsb.edu

25 **Abstract**

26 African elephants (*Loxodonta africana*) are the largest extant terrestrial mammals, with bodies
27 containing enormous quantities of nutrients. Yet we know little about how these nutrients move
28 through the ecosystem after an elephant dies. Here, we investigated the initial effects (1-26
29 months post-death) of elephant megacarcasses on savanna soil and plant nutrient pools in Kruger
30 National Park, South Africa. We hypothesized that: (H1) elephant megacarcass decomposition
31 would release nutrients into soil, resulting in higher concentrations of soil nitrogen (N),
32 phosphorus (P), and cations near the center of carcass sites; (H2) carbon (C) inputs to the soil
33 would stimulate microbial activity, resulting in increased soil respiration potential near the center
34 of carcass sites; and (H3) carcass-derived nutrients would be absorbed by plants, resulting in
35 higher foliar nutrient concentrations near the center of carcass sites. To test our hypotheses, we
36 identified 10 elephant carcass sites split evenly between nutrient-poor granitic and nutrient-rich
37 basaltic soils. At each site, we ran transects in the four cardinal directions from the center of the
38 carcass site, collecting soil and grass (*Urochloa trichopus*, formerly *U. mosambicensis*) samples
39 at 0, 2.5, 5, 10, and 15 m. We then analyzed samples for CNP and cation concentrations and
40 quantified soil microbial respiration potential. We found that concentrations of soil nitrate,
41 ammonium, $\delta^{15}\text{N}$, phosphate, and sodium were elevated closer to the center of carcass sites (H1).
42 Microbial respiration potentials were positively correlated with soil organic C, and both
43 respiration and organic C decreased with distance from the carcass (H2). Finally, we found
44 evidence that plants were readily absorbing carcass-derived nutrients from the soil, with foliar
45 %N, $\delta^{15}\text{N}$, iron, potassium, magnesium, and sodium significantly elevated closer to the center of
46 carcass sites (H3). Together, these results indicate that elephant megacarcasses release
47 ecologically consequential pulses of nutrients into the soil that influence soil microbial activity

48 and are absorbed by plants into the above-ground nutrient pools. These localized nutrient pulses
49 may drive spatiotemporal heterogeneity in plant diversity, herbivore behavior, and ecosystem
50 processes.

51 **Sect. 1 Introduction**

52 Living animals affect nutrient flows through ecosystems (Schmitz et al. 2018), but we have only
53 recently acknowledged that the nutrients from animal carcasses could also influence ecosystem
54 processes (Barton et al. 2013; Monk et al. 2024). In marine ecosystems, whale carcasses function
55 as unique hotspots of nutrient cycling, biodiversity, and ecosystem processes (Roman et al.
56 2014). In terrestrial systems, mass mortality events (e.g., wildebeest, cicadas) create nutrient
57 hotspots (Yang, 2004; Subalusky et al. 2020), while individual small and medium-sized
58 carcasses release pulses of nutrients into the soil (Town, 2000; Barton et al. 2016; Olea et al.
59 2019). Yet, terrestrial ecosystem ecology lacks knowledge about the role of megacarcasses
60 (carcasses of animals such as elephants and rhinoceros that are >1000 kg at death) as potential
61 drivers of spatiotemporal heterogeneity in nutrient cycling and ecosystem processes. Importantly,
62 these megacarcasses may be functionally different than smaller carcasses due to the
63 extraordinarily high concentration of nutrients and residence time of the decomposing animal
64 (see reviews by Barton et al. 2013; Barton, 2016; Barton & Bump 2019). This question around
65 the role of megacarcasses is particularly relevant given the megaherbivore losses that occurred
66 during the Pleistocene extinctions and that are still occurring today (Ripple et al. 2015). We are
67 only beginning to understand how the ‘extinction aftershock’ of losing the largest species
68 impacts ecosystems (Owen-Smith, 1989; Flannery, 1990), and no study has yet investigated how
69 the loss of megacarcasses might influence the dynamics of terrestrial ecosystems (Doughty et al.
70 2013; Doughty et al. 2016).

71 We can only evaluate the importance of terrestrial megacarcasses for nutrient cycling in
72 ecosystems where megaherbivores still exist, such as African savannas. The African savanna
73 elephant (*Loxodonta africana*) is the largest extant land animal and is known for its key

74 ecological effects in savannas while alive (e.g., dispersing seeds, creating plant refuges,
75 preventing woody encroachment) (Skarpe et al. 2004; Asner et al. 2009; Campos-Arceiz &
76 Blake, 2011; Coverdale et al. 2016; Guy et al. 2021). Yet, the elephant's large body mass may
77 mean that it also has an outsized impact in these ecosystems even after death. A 4000-kg
78 elephant megacarcass likely represents ~2000 kg carbon (C), ~300 kg nitrogen (N), and ~125 kg
79 phosphorus (P) deposited in the savanna landscape (estimated from stoichiometry of elephants
80 and other mammals in Sterner & Elser, 2002). The N deposition from one elephant megacarcass
81 (in a 700 m² impact zone assuming a 15 m disturbance radius) is roughly equivalent to the N
82 delivered to 10,000 m² of savanna from ~100 years from atmospheric deposition (Mphepya et al.
83 2006).

84 If megacarcasses provide large nutrient pulses, then they likely create hotspots of
85 important below- and aboveground processes. Belowground, soil respiration and organic matter
86 decomposition might increase with nutrient inputs from carcasses (Risch et al. 2020).
87 Concentrations of C, N, P, and potassium (K) are often elevated near carcasses of medium-sized
88 animals (e.g., bison, moose, kangaroo, vicuña) (Towne, 2000; Bump et al. 2009a; Macdonald et
89 al. 2014; Risch et al. 2020; Monk et al. 2024), and nutrients such as P and calcium (Ca) continue
90 leaching from bones even after soft tissues have been consumed or degraded (Coe, 1978; Keenan
91 & Beeler, 2023). Aboveground, plant growth in African savannas is strongly limited by nutrient
92 availability, most commonly N and P, but also by cations such as Ca, K, and magnesium (Mg)
93 (Jobbágy & Jackson, 2004; Ries & Shugart, 2008; Pellegrini, 2016), and there is evidence of
94 cation limitation of plants (particularly K⁺ and Ca²⁺) on African savannas (Lathwell & Grove,
95 1996; Agbenin & Yakubu, 2006). Thus, the large influx of nutrients released from
96 megacarcasses might increase the mobilization of nutrients by plants, potentially increasing

97 nutrient accessibility for vertebrate and invertebrate herbivores (Yang, 2008; Grant & Scholes,
98 2006; Anderson et al. 2010; Joern et al. 2012). Indeed, carcasses of smaller vertebrates (e.g.,
99 salmon, deer) can increase the proportions of nitrogen and $\delta^{15}\text{N}$ (an indicator of animal-driven N)
100 in plants within just a few months post-death (Hocking & Reynolds, 2012; van Klink et al.
101 2020).

102 To assess the effects of megacarcasses on local nutrient pools (Figure 1), we measured
103 the initial contributions of elephant carcasses (1-26 months post-death) to soil and plant nutrients
104 in the Kruger National Park (KNP), South Africa. Further, we examined the effects of elephant
105 carcasses on the two main soil types in KNP: sandy, relatively nutrient-poor granitic soils and
106 clayey, relatively nutrient-rich basaltic soils (Venter et al. 2003). At each site, we ran transects in
107 each cardinal direction from the center of the site where an elephant died, collecting samples of
108 soil and a palatable grass species (*Urochloa trichopus*) at 0, 2.5, 5, 10, and 15 m. We then
109 analyzed soil samples for CNP and cation content, quantified soil microbial respiration potential,
110 and measured %N, $\delta^{15}\text{N}$, and macro- and micronutrient content in grass tissue. We hypothesized
111 that: (H1) elephant megacarcass decomposition would release nutrients into soil, resulting in
112 higher concentrations of soil N, P, and cations near the center of carcass sites; (H2) C inputs to
113 the soil would stimulate microbial activity, resulting in increased soil respiration potential near
114 the center of carcass sites; and (H3) carcass-derived nutrients would move from soil into plants,
115 resulting in higher foliar nutrient concentrations near the center of carcass sites. We predicted
116 that enrichment effects from megacarcasses would be greater on sites with fresher carcasses
117 relative to older carcasses and on nutrient-poor granitic sites compared to nutrient-rich basaltic
118 sites.

119

120 **Sect. 2 Methods**

121 **2.1 Study system and sample collection**

122 We performed this research in the southern part of the Kruger National Park (KNP), South
123 Africa (24.996 S, 31.592 E, ~275m elevation). The two dominant soil types in KNP are granitic
124 soils (inceptisols) and basaltic soils (versitols or andisols) (Khomo et al. 2017). The clay-rich
125 basaltic soils have relatively large surface area, enabling them to retain larger quantities of water
126 than granitic soils, which drain water more quickly and therefore are lower in water-soluble
127 nutrients (Buitenwerf, Kulmatiski, & Higgins, 2014; Rughöft et al. 2016). The landscape of
128 KNP is a mix of savanna grasslands and broadleaf woodlands, with an overstory dominated by
129 trees from the genus *Combretum* (red bushwillow, *C. apiculatum*; russet bushwillow, *C.*
130 *hereroense*; leadwood, *C. imberbe*) and trees formerly known as acacias (knobthorn,
131 *Senegalsensis nigrescens*; umbrella thorn, *Vachellia tortillis*). The park hosts a full suite of
132 African savanna animals, including ~30,000 elephants (*Loxodonta africana*) (Coetsee &
133 Ferreira, 2023), with a mortality rate of ~2% (~600 elephants per year). The targeted region of
134 KNP has a high density of scavengers and predators, including white-backed vultures (*Gyps*
135 *africanus*), spotted hyenas (*Crocuta crocuta*), and lions (*Panthera leo*) (Owen-Smith & Mills,
136 2007).

137 During the wet season in March 2023, we identified ten elephant carcass sites (1-26
138 months post-death), five on relatively nutrient-rich basaltic soil and five on nutrient-poor granitic
139 soil. KNP section rangers provided precise GPS locations of where elephant carcasses had been
140 found. Most elephants died of old age, illness, injury, or, in the case of one young bull, fighting
141 over territory. Carcass sites were recognizable *in situ* by a persistent bonefield, undigested gut
142 contents, and an absence of herbaceous vegetation. At each site, we hammered a rebar post into

143 the center of the megacarcass disturbance and ran 15 m transects out from the post in each of the
144 four cardinal directions. We collected green leaf material from *U. trichopus*, a common and
145 abundant palatable grass species, and used an auger to collect soil samples to a depth of 10 cm at
146 five points along each transect (0.5, 2.5, 5, 10, and 15 m) (Bump, Peterson, & Vucetich, 2009;
147 Holdo & Mack, 2014; Gray & Bond, 2015; Monk et al. 2024). We treated the 10-15m distances
148 as representative of background concentrations of nutrients based on pilot data showing that the
149 effect of elephant carcasses on soil nutrient concentrations was undetectable at this distance
150 away from the carcass site, similar to studies on the carcasses of other large vertebrates (e.g.,
151 Towne, 2000; Bump et al. 2009). We pooled and homogenized the samples to yield one
152 composite leaf and one composite soil sample per sampling distance from each carcass site. Soil
153 samples were sieved in a 5-mm metal sieve which was cleaned in between samples with 70%
154 ethanol. Soil samples were stored in a cooler during fieldwork. On the day they were collected,
155 we used 5 g of each soil sample for soil respiration measurements (described below). The rest of
156 each sample was stored in plastic bags in a -20°C freezer until nutrient analyses; they were stored
157 in coolers with ice blocks during the transition from the freezer at the field site to the freezers at
158 the labs. We chose to freeze samples rather than storing at room temperature based on literature
159 demonstrating that the impacts of freezing on soil nitrate and ammonium concentrations are
160 fairly minimal, except in specific cases of high soil acidity or peaty soils that were not present at
161 our field site (Esala, 1995; Turner & Romero, 2009; Sollen-Norrlin & Rintoul-Hynes, 2024).
162 Leaf samples were stored in paper bags at room temperature until dried for analyses (see below).

163

164 **2.3 Hypothesis testing**

165 We tested our first hypothesis that elephant carcass decomposition would release nutrients into
166 the soil by performing soil nutrient analyses. We sent 250 g of each soil sample to Eco-Analytica
167 laboratory at the North-West University in Potchefstroom, South Africa for measurements of soil
168 concentrations of ammonium $[\text{NH}_4]^+$, nitrate $[\text{NO}_3]^-$, phosphate $[\text{PO}_4]^{3-}$, and plant-available P.
169 Samples were air-dried and sieved through $< 2\text{mm}$ mesh prior to chemical analysis. Plant-
170 available P was extracted from 4 g of soil and 30 ml extraction fluid (1:7.5 ratio) using an acid-
171 fluoride solution (P Bray-1), measured colorimetrically using a Systea EasyChem200 analyser,
172 and expressed as mg/kg. The detection limit was 0.5 mg/kg, and plant available P measurements
173 < 0.5 mg/kg were replaced with half the detection limit (0.25 mg/kg) (Croghan & Egeghy, 2003;
174 Keenan & Beeler, 2023). Water-soluble nitrate and phosphate anions were extracted from
175 volume on volume 100 ml soil and 200 ml deionized water, analyzed by ion chromatography on
176 a Metrohm 930 Compact Flex System, and measured as mg/L. Ammonium (also 1:2 water
177 extract) was analyzed colorimetrically using a Systea EasyChem200 analyzer and measured as
178 mg/L. Detection limits for soil ions were 0.01 mg/L, and soil ion concentrations measured as
179 < 0.01 mg/L were replaced with half the detection limit (0.005 mg/L). To convert the nitrate,
180 ammonium, and phosphate units from mg/L to mg/kg, we multiplied by 2, based on the 1:2 soil
181 to water extraction ratio.

182 To determine whether soil anions were distinct and elevated at the center of carcass sites
183 relative to soil further from the center, concentrations of sodium (Na), magnesium (Mg), iron
184 (Fe), calcium (Ca), potassium (K), and phosphorus (P) cations were measured using microwave-
185 assisted digestion. Air-dried and sieved (> 2 mm) soil samples, weighed to 0.2 g, were
186 microwaved in 9 ml 65% nitric acid (HNO_3) and 3 ml 32% hydrochloric acid (HCl) according to
187 EPA 3051b in a Milestone, Ethos microwave digester with UP, Maxi 44 rotor. A period of 20

188 minutes allowed the system to reach 1800 MW at a temperature of 200 °C which was maintained
189 for 15 minutes. After cooling, the samples were brought up to a final volume of 50 ml and
190 analyzed on an Agilent 7500 CE ICP-MS fitted with CRC (Collision Reaction Cell) technology
191 for interference removal. The instrument is optimized using a solution containing Li, Y, Ce, and
192 Tl (1 ppb) for standard low-oxide/low interference levels ($\leq 1.5\%$) while maintaining high
193 sensitivity across the mass range. The instrument was calibrated using ULTRASPEC® certified
194 custom mixed multi-element stock standard solutions containing all the elements of interest (De
195 Bruyn Spectroscopic Solutions, South Africa). Calibrations spanned the range of 0 – 30 ppm for
196 the mineral elements Ca, Mg, Na, and K and 0 – 0.3 ppm for the rest of the trace elements.
197 Elemental concentrations were expressed as mg/kg.

198 Finally, to determine whether elevated N levels in soils were derived from the carcass, we
199 sent 10 g of each sample to the BIOGRIP laboratory within the Central Analytical Facility at
200 Stellenbosch University for measurements of soil %N and $\delta^{15}\text{N}$, obtained using a Vario Isotope
201 Select Elemental Analyzer connected to a thermal conductivity detector and an Isoprime
202 precisions isotope ratio mass spectrometer (IRMS). Samples were oven-dried at 60°C for 48
203 hours and milled to a fine powder using a Retsch MM400 mill (Germany). The powdered
204 samples were weighed (2 – 60 mg) prior to combustion at 950°C. The gasses were reduced to N_2
205 (undiluted) in the reduction column, which was held at 600°C. A high organic carbon (HOC) soil
206 standard ($0.52 \pm 0.02\%$ N), along with two international reference standards (USGS40 ($\delta^{15}\text{N} -$
207 4.52% AIR) and USGS41 ($\delta^{15}\text{N} +47.57\%$ AIR)) were used for calibration. The N elemental
208 content was expressed relative to atmospheric N as N_2 $\delta^{15}\text{NAIR}$ (‰). The quantification limit for
209 $\delta^{15}\text{N}$ on the IRMS is 1 nA (nanoAmp), and the quantification limit for %N is 0.06%. The

210 precision for %N was 0.02% and for $\delta^{15}\text{N}$ is $\pm 0.11\%$, determined using the HOC standard, which
211 was run multiple times throughout the analysis.

212 To test our second hypothesis that nutrient inputs to the soil would stimulate microbial
213 activity, we measured soil organic C, water content, and microbial respiration potential. We sent
214 10 g of each sample to the BIOGRIP laboratory for measurements of soil organic C using a
215 Vario TOC Cube (Elementar, Germany). Samples (dried and milled as above) were weighed (10
216 – 60 mg), acidified using 10% HCl to remove the total inorganic C (carbonates), and dried
217 overnight at 60°C. All samples were analyzed through combustion at 950°C. The released CO₂
218 was measured by a non-dispersive infrared (NDIR) sensor. A high organic C ($7.45 \pm 0.14\%$ C)
219 soil standard from Elemental Microanalysis Ltd (UK) was included during the analysis. The
220 quantification limit for %C is 0.14%. The precision for the %C was 0.09% and was determined
221 using the low organic C (LOC) standard ($1.86 \pm 0.14\%$ C), which was run multiple times
222 throughout the analysis.

223 To quantify soil respiration and water content, we used an incubation method (Lemoine
224 et al. 2023) in which 5 g (± 0.2 g) of each sample was placed into a 100 ml clear glass bottle,
225 sealed, and flushed with CO₂-free air. Following flushing, we incubated the bottles for one hour
226 at 25°C. We then recorded CO₂ concentrations using an LI-850 CO₂/H₂O infrared gas analyzer.
227 After soil respiration measurements, we determined sample dry weight by drying each sample at
228 60°C for 24-48 hours until stable mass was achieved. We subtracted dry weight from starting
229 weight to obtain soil water content. Finally, we used the dry weights and the Ideal Gas Law to
230 standardize all respiration measurements to CO₂ $\mu\text{g h}^{-1}\text{g dry soil}^{-1}$.

231 To test our third hypothesis that carcass-derived nutrients would be incorporated by
232 plants, we measured foliar nutrient concentrations in *U. trichopus*. Two grams of each dried leaf

233 sample was sent to the BIOGRIP laboratory for preparation and measurements of %N and $\delta^{15}\text{N}$
234 via stable isotope analysis as described above. A Sorghum flour standard (1.47 ± 0.25 %N) from
235 Elemental Microanalysis Ltd (UK) was used for calibration, along with two international
236 reference standards (USGS40 and USGS41). The quantification limit for $\delta^{15}\text{N}$ on the IRMS is 1
237 nA, and the quantification limit for %N is 1.3%. The precision for the %N was 0.02% and for
238 $\delta^{15}\text{N}$ is $\pm 0.08\%$. Limits were determined using the sorghum flour standard, which was run
239 multiple times throughout the analysis. Additionally, we sent 5 g per sample to Cedara
240 Analytical Services Laboratory to quantify micronutrients in grass tissue (P, Na, Mg, K, Ca, and
241 Fe) using Inductively Coupled Plasma Optical Emission Spectroscopy (ICP-OES 5800, Agilent,
242 USA). Samples were dried (110°C overnight) and milled to a fine powder. Subsamples (0.5 g)
243 were ashed at 450°C for 4 hours, and the ash was re-wet using 2 mL conc. HCl (32%). Samples
244 were evaporated to dryness then re-suspended in 25 mL 1M HCl before filtering. Lastly, the
245 filtrate was diluted with de-ionized water in a ratio of 5:20 filtrate to water. To calibrate the ICP-
246 OES, solutions containing known amounts of each element were measured (10-20 ppm for Na
247 and C, 200-1500 ppm for Fe, 0.5-3.75% for K, and 0.125-0.5% for P), prepared from 1000 ppm
248 primary single standards. At three of the ten sites, we did not find sufficient plant material at the
249 central point for analysis, resulting in a sample size of $N = 7$ for the center (distance = 0.5m)
250 measurement for leaf nutrient analyses.

251 To test whether each response variable for the three hypotheses was significantly
252 associated with soil type and/or distance from the carcass center, we performed a model selection
253 procedure. For each response variable, we ran five generalized linear mixed models using the
254 gamma family (link = log) in the package *lme4* (Bates et al. 2015): (i) soil type + distance + soil
255 type \times distance interaction, (ii) soil type + distance, (iii) soil type, (iv) distance, and (v) a null

256 model indicating no significant difference in slope or intercept after accounting for carcass site.
257 All models included carcass site as a random effect to account for individual variation. Each
258 model included 50 observations (10 sites x 5 distances per site). For samples in which the
259 nutrient level was listed as 0 or undetectable, we accounted for the uncertainty by using half the
260 detection level as described above. The narrow distribution of ages (1-26 months since death)
261 with the sample size of $N = 10$ sites made testing for the effect of age challenging, so we did not
262 include carcass age in the models. We compared the models for each response variable using
263 Akaike Information Criterion (AICc). Models with a $\Delta AICc \leq 2$ were considered roughly
264 equivalent in fit (Burnham and Anderson, 2002).

265 In addition to these models, for our second hypothesis we regressed soil respiration
266 potential against soil organic C, expecting that the two would be positively correlated. We ran a
267 generalized linear mixed model with soil respiration potential as the response variable. The
268 model included soil organic C + distance + soil type, with carcass site as a random effect. We did
269 not include an interaction with soil type in this model due to sample size restrictions. Respiration
270 potential and organic C were both log-transformed to achieve normality.

271 To determine whether leaf and soil micronutrient composition differed with distance and
272 soil type, we ran permutational analysis of variance (perMANOVA) in *vegan* (Oksanen et al.
273 2022). We ran the same model separately for soil and leaf micronutrient composition (soil type +
274 distance). To determine which micronutrients contributed most to compositional differences
275 across distances and soil types, we calculated samplewise Bray-Curtis dissimilarity and
276 performed principal component analysis. We also tested for differences in variance in
277 micronutrient composition across distances and soil types using “betadisper” in *vegan* (Oksanen

278 et al. 2022). We ran linear models to test for correlations between leaf and soil concentrations of
279 each micronutrient. Each model included distance as a covariate and site as a random effect.

280 Finally, to test the impact of carcass age on key soil metrics, we ran exponential decay
281 functions for soil ammonium, nitrate, phosphate, and respiration verses carcass age for samples
282 from the center of the carcass site (0.5m sampling location). We also performed a t-test to verify
283 that there was no difference in mean carcass age across soil types.

284 All statistical analyses were performed in R version 4.2.1 (R Core Team, 2022).

285

286 **Sect. 3 Results**

287 **3.1 Hypothesis 1: Effects of megacarcasses on soil nutrient pools**

288 We found partial support for our first hypothesis that soil N and P concentrations would be
289 higher closer to the center of carcass sites (Table S1). Soil %N (Figure 2A) was overall greater in
290 basaltic soils, and it decreased with distance from the carcass site on granitic soils. Soil nitrate
291 (Figure 2B) decreased with distance from the carcass site but did not differ between soil types.
292 Ammonium (Figure 2C) also decreased with distance, but only in granitic soils. $\delta^{15}\text{N}$ (Figure 2D)
293 was greater in granitic soils and decreased with distance in both soil types, indicating that the
294 proportion of animal-sourced N in the soil was greater near the center of the carcass site. Soil
295 phosphate, plant available P, and mineral P (Figure 2E-G) all exhibited significant soil \times distance
296 interactions. Phosphate (Figure 2E) was highly elevated at the center of carcass sites and
297 decreased steeply with distance, but only in granitic soils. Plant-available P (Figure 2F)
298 decreased with distance in both soil types, but the effect was strongest in granitic soils. Finally,
299 mineral P (Figure 2G) was greater in basaltic soils, and there was a small decrease with distance
300 in granitic soils but not in basaltic soils.

301 Contrary to our first hypothesis, soil cation composition did not differ significantly with
302 distance from the carcass center; nor did most individual cations (Table S1). The perMANOVA
303 results showed that soil cation composition did not differ significantly with distance ($R^2 = 0.00$,
304 $F_{4,44} = 0.0$, $P = 1.000$) (Figure S2A), but it did differ significantly with soil type ($R^2 = 0.71$, $F_{1,44}$
305 $= 108.8$, $P = 0.001$) (Figure S2B). There was no significant difference in variance with distance
306 ($F_{4,45} = 0.0$, $P = 0.996$) or soil type ($F_{1,48} = 2.6$, $P = 0.115$). Principal components analysis
307 showed that dimension 1 explained 53.6% of the variation between soil types and was driven
308 primarily by differences in Mg, Ca, and Fe. Dimension 2 explained 25.9% of variation and was
309 driven primarily by differences in K. Soil Na (Figure S3A) was marginally greater in granitic
310 soils and decreased with distance from the carcass, with the effect greater in granitic soils. Soil K
311 (Figure S3B) was greater in basaltic soils and decreased marginally with distance. Soil Fe, Mg,
312 and Ca (Figure S3C-E) were greater in basaltic soils, with minimal effects of distance.

313

314 **3.2 Hypothesis 2: Effects of megacarcasses on soil carbon and respiration**

315 Consistent with our second hypothesis, soil respiration potential was marginally positively
316 correlated with soil organic carbon concentration and decreased significantly with distance but
317 did not differ with soil type (Figure 3). We found no evidence for differences in soil water
318 content (Figure S4A) or soil pH (Figure S4B) with distance or soil type. In both cases, the null
319 ranked among the set of top models (Table S1).

320

321 **3.3 Hypothesis 3: Effects of megacarcasses on plant nutrient pools**

322 Consistent with our third hypothesis, we found elevated foliar nutrient concentrations in *U.*
323 *trichopus* at elephant carcass sites. Leaf %N (Figure 4A) and $\delta^{15}\text{N}$ (Figure 4B) both decreased

324 with distance from the carcass center. $\delta^{15}\text{N}$ exhibited a significant soil \times distance interaction in
325 which it was overall greater in basaltic soils, but the difference between the two soil types was
326 greater closer to the carcass site. Foliar P was greater in basaltic soils and decreased only
327 marginally with distance in the granite soils. Finally, the foliar N:P ratio was greater in granitic
328 soils and decreased with distance in the basaltic soils.

329 Leaf micronutrient composition did not differ significantly with distance ($R^2 = 0.13$, $F_{4,40}$
330 $= 1.9$, $P = 0.062$; Figure S5A) but did differ with soil type ($R^2 = 0.17$, $F_{1,40} = 9.7$, $P = 0.001$;
331 Figure S5B). There was no significant difference in variance with distance ($F_{4,41} = 0.5$, $P =$
332 0.713) or soil type ($F_{1,44} = 1.9$, $P = 0.173$). Dimension 1 explained 42.8% of the variance across
333 soil types and was primarily driven by Mg, Na, and P. Dimension 2 explained 26.6% of the
334 variance and was driven mainly by K, Ca, and Fe. Foliar Na (Figure S6A) and Mg (Figure S6B)
335 were both greater in basaltic soils and decreased with distance from the carcass center. Foliar K
336 (Figure S6C) and Fe (Figure S6D) both decreased with distance as well but did not differ with
337 soil type. The null model was in the top set for foliar Ca, indicating no significant relationship
338 between foliar Ca concentrations and soil type or distance from the carcass center. Individual
339 micronutrients (K, Ca, Mg, Fe) were not correlated between leaf and soil samples, with the
340 exception of Na (Table S3).

341

342 **3.4 Effects of carcass age on soil ions and respiration potential**

343 Soil ammonium ($\alpha = 0.018$, $P < 0.001$), phosphate ($\alpha = 0.023$, $P < 0.001$), and respiration
344 potential ($\alpha = 0.058$, $P < 0.001$) all decreased significantly with carcass age (Figure 5A-C). The
345 exponential decay model for nitrate failed to converge due to an outlier with extremely high soil
346 nitrate (1454 mg/kg) at 258 days post-death (Figure 5D). We ran a t-test to test for a difference in

347 mean carcass age between soil types and found no significant difference between the two groups
348 ($P = 0.294$).

349

350 **Sect. 4 Discussion**

351 Here, we show that elephant megacarcasses influence soil and foliar nutrients during at least the
352 first two years following mortality. Consistent with our hypotheses, soil nitrate (Figure 2B),
353 ammonium (Figure 2C), $\delta^{15}\text{N}$ (Figure 2D), and P (Figure 2E-F) concentrations were all elevated
354 at the center of carcass sites and decreased with distance from the center. Soil %N, nitrate,
355 ammonium, and plant-available P concentrations at the 15m point were consistent with those
356 found in other studies of soil nutrient content in Kruger (Aranibar et al. 2003; Rughöft et al.
357 2016), confirming that the 15m point serves as an effective baseline control in this experiment.
358 Microbial respiration potential was also elevated towards the center of carcass sites and was
359 correlated with the abundance of organic C (Figure 3). Finally, %N (Figure 4A) and $\delta^{15}\text{N}$ in a
360 common grass (Figure 4B) were both elevated closer to the centers of carcass sites compared to
361 grass farther from carcasses. Together, these results indicate that carcass-derived nutrients move
362 into soil and subsequently get absorbed by plants over relatively short time scales, cycling
363 essential nutrients such as N from carrion into the soil and then back into aboveground nutrient
364 pools.

365 The initial influx of ammonium from elephant carcasses is consistent with literature on
366 smaller carrion but much greater in magnitude in these much larger carcasses (Parmenter &
367 McMachon, 2009; Quaggiotto et al. 2019; Yong et al. 2019). The mean ammonium level at the
368 center of carcass sites (17.4 mg/L) was 5x the level generally considered toxic to plants (3.5
369 mg/L; Britto & Kronzucker, 2002). Yet, we found living grass—typically *U. trichopus*—in the

370 center of the carcass site at seven out of ten of our sites (ammonium range 5-86 mg/L) and at the
371 2.5m distance for all sites (ammonium range 0-36 mg/L). The three sites without vegetation in
372 the center had the highest ammonium levels (35-72 mg/L), suggesting that *U. trichopus* has a
373 higher degree of ammonium tolerance than some sympatric grass species but may still be limited
374 by the extreme ammonium levels at the centers of these three relatively fresh carcass sites.
375 However, the recentness of the disturbance from the carcass likely also plays a role in
376 determining plant abundance near the center of the carcass. These results indicate that
377 ammonium remains elevated at elephant carcass sites for at least the first two years post-death
378 and may reduce, but not eliminate, plant growth over this time period.

379 Soil nitrate (Figure 2B) and soil respiration potential (Figure 3) were also elevated near
380 the center of carcass sites, indicating higher rates of activity of heterotrophic microbes (Prosser,
381 2011). These results are consistent with other work on carrion, where microbial activity tends to
382 be greater in soils near carcasses as compared to surrounding soil (Bump et al. 2009b). However,
383 carcass effects on soil microbial respiration exhibit a high degree of intra-system variation (Risch
384 et al. 2020), and the potentially short window during which increased respiration occurs may
385 make capturing these variations challenging. For example, soil respiration potential at the center
386 of the three youngest carcass sites was on average 2x higher than the seven older sites (18.43 and
387 9.62 $\mu\text{g CO}_2/\text{hr}$, respectively; Figure 5D). Thus, the impact of increased organic C on soil
388 microbial processes may be relatively short lived and only last a matter of months (Keenan et al.
389 2018; Keenan, Schaeffer, & DeBruyn, 2019). These trends are consistent with soil ammonium
390 and phosphate, both of which are highest at the youngest carcass sites (<200 days post death;
391 Figure 5A-B). Soil microbial respiration rate is also highly elevated early on, but it decreases at a
392 faster rate over time than soil ions (Figure 5C). Thus, soil dynamics during the first several

393 months after death may play a crucial role in determining the long-term impacts of
394 megacarcasses on savannas and therefore provides a promising avenue for future research.

395 Elevated soil phosphate (Figure 2E) and plant-available P (Figure 2F) at the center of
396 carcass sites were also consistent with expectations from the literature (Bump et al. 2009a;
397 Parmenter & MacMahon, 2009). However, elevated P levels in soil did not translate to elevated
398 P in grass leaves (Figure 4C), which could suggest a lag between trends in soil and plants that is
399 longer for P than for N. This lag could occur because phosphate easily forms chemical bonds
400 with other soil ions (e.g., iron and aluminum in acidic soils and calcium in basic soils). Nitrate
401 does not form these bonds and therefore has greater water solubility and mobility in soils and
402 may be more readily taken up by plants (Wiersum, 1962; Arai & Sparks, 2007). However, it is
403 also possible that P limitation in Kruger is not as strong as it is in some other African savanna
404 systems (Pellegrini, 2016). The foliar N:P ratios measured in this experiment were higher closer
405 to the center of the carcass site (median 9.38 at 0 m and 4.83 at 15 m), indicating that N
406 limitation may be relatively stronger further from the carcass site, and P limitation may be
407 relatively stronger closer to the center (Figure 4D, Table S2). These relatively high foliar N:P
408 ratios at the center of carcass sites are similar to those found in N fertilization studies in Kruger
409 (Craine et al. 2008), further supporting the idea that the influx of N from megacarcasses may
410 shift the soil from relatively more N limited to more P limited.

411 The elevated plant-available P at the center of carcass sites likely came primarily from
412 phosphate released from decomposing tissue (Yong et al. 2019). Bone decomposition, which is
413 also likely a major source of P from animal carcasses (Subalusky et al. 2020), occurs over long
414 time scales (Coe, 1978; Subalusky et al. 2020) and therefore should result in the slow release of
415 P and a gradual decrease in the N:P ratio (Parmenter & MacMahon, 2009; Quaggiotto et al.

416 2019). Indeed, initial inorganic N influxes to the Mara River in Kenya from mass wildebeest die-
417 offs are 10-fold greater than concurrent increases in P, which instead releases slowly over about
418 seven years of bone decomposition (Subalusky et al. 2017). Research following megacarcasses
419 over longer timeframes post-death is needed to clarify when P from enriched soil is absorbed by
420 plants and at what stage megacarcass bones begin contributing to soil P dynamics. It is also
421 possible that bone dispersal by scavengers may result in less P leaching from bones close to
422 where the elephant died and more P being distributed across the landscape at distances far from
423 the carcass site.

424 The contributions of megacarcasses to soil macronutrient and cation pools were strongly
425 associated with soil type. Our results confirmed the previously-established trend that basaltic
426 soils are overall more cation rich than granitic soils, with greater concentrations of P, K, Fe, Mg,
427 and Ca (Figure 2G; Figure S3B-E; Gertenbach, 1983; Craine, Morrow, & Stock, 2008; Wigley et
428 al. 2014). However, soil ammonium, $\delta^{15}\text{N}$, and phosphate were all higher in the granitic soils
429 towards the center of carcass sites, decreasing steeply to be similar to basaltic soils about 10 m
430 from the carcass center (Figure 2C-E). These results indicate that the impact of organic matter
431 from megacarcasses may be stronger in relatively nutrient-poor and sandy granitic soil compared
432 with nutrient-rich and clayey basaltic soil. We were surprised that grass on basaltic soil did not
433 consistently exhibit greater concentrations of cations and macronutrients. One potential
434 explanation is that grass may primarily be limited by macronutrients like N and P on both soil
435 types (Craine et al. 2008; Holdo, 2013) rather than by cations. Thus, even with increased cation
436 availability their actual uptake may not differ substantially. Studies on ungulate carcasses (e.g.,
437 muskoxen, moose, zebra) have shown increased foliar N at carcass sites (Danell et al. 2002;
438 Bump et al. 2009b; Turner et al. 2014), but to date there is little research on the flow of cations

439 from carrion to plants and none on the pipeline from megacarcasses to plants. Moreover, it
440 remains to be seen whether increases in foliar N and other nutrients affect herbivory rates at
441 carcass sites and how long such effects may last.

442 The magnitude of nutrient inputs from megacarcasses, as well as the substantial size and
443 duration of their impact zones, means their impacts on ecosystem processes may be functionally
444 distinct from smaller carrion. Indeed, there is evidence that carcass size strongly impacts
445 scavenger food web structure (Moleón et al. 2015; Morris et al. 2023). Moreover, the attraction
446 of animals to carcasses via scavenging, predation, or mourning (Goldenberg & Wittemyer, 2020)
447 could have positive feedbacks on nutrient cycling (Bump, Peterson, & Vucetich, 2009; Monk et
448 al. 2024), which may be magnified by carcass size. Thus, the impacts of megacarcasses on
449 savanna ecosystem processes may be dissimilar to the effects of small carrion and more similar
450 to other more persistent contributors to savanna ecosystem processes, such as termite mounds
451 (Davies et al. 2016), cattle bomas (Augustine, 2003), and even mass animal mortality events
452 (Subalusky et al. 2017, 2020).

453

454 **Sect. 5 Conclusions**

455 This study is an important first step in understanding the ecological legacies of megacarcasses on
456 savanna ecosystem processes. During the first two years post-death, elephant carcasses released
457 pulses of ammonium, nitrate, and phosphate, all of which influence savanna primary
458 productivity. These nutrients stimulated soil microbial activity and enriched foliar N, and the
459 effects were strongest in nutrient-poor soil, with potential long-term impacts on savanna nutrient
460 heterogeneity. These carcass-derived nutrient hotspots represent a previously unstudied function

461 of megaherbivores on savannas—one that we need to better understand in order to comprehend
462 the full impacts of megaherbivore population declines in the Anthropocene.

463

464 **Data and Code Availability:** Data and computer code are archived on Dryad Digital Repository
465 (<https://doi.org/10.5061/dryad.wpzgmsbwm>).

466

467 **Author Contributions:** Deron E. Burkepile, Nathan P. Lemoine, Izak P. J. Smit, Tercia
468 Strydom, Aimee Tallian, Johan T. du Toit, Dave I. Thompson, and Joshua P. Schimel conceived
469 the study. Michelle L. Budny, Johan T. du Toit, Nathan P. Lemoine, Joshua P. Schimel, Izak P.
470 J. Smit, Tercia Strydom, Aimee Tallian, Dave I. Thompson, Helga van Coller, and Deron E.
471 Burkepile collected samples. Courtney G. Reed, Nathan P. Lemoine, Dave I. Thompson, and
472 Deron E. Burkepile analyzed the data. Courtney G. Reed drafted the manuscript, and all authors
473 contributed to editing.

474

475 **Competing Interests:** The authors declare that they have no conflict of interest.

476

477 **Acknowledgments:** Funding for this research was provided by the National Science Foundation
478 (#s 2128092, 2128093, and 2128094) and the University of California Santa Barbara Academic
479 Senate. All research was completed under permits from South African National Parks (SS554).
480 We thank the field assistants of SANParks for guiding and protection in the field, as well as the
481 section rangers and Sandra Snelling for GPS locations and ages of carcasses. We thank Mr.
482 Lucky Sithole (Cedara Analytical Services Laboratory), Ms. Terina Vermeulen (Eco-Analytica
483 Laboratory), and Dr. Janine Colling (BIOGRIP laboratory) for extensive laboratory support.

484 Select data used in this research paper were generated using equipment in the DSI funded
485 BIOGRIP soil and water node at Stellenbosch University.

486

487 **References**

- 488 1. Agbenin, J. O. & Yakubu, S. Potassium-calcium and potassium-magnesium exchange
489 equilibria in an acid savanna soil from northern Nigeria. *Geoderma*, 136, 542-554,
490 <https://doi.org/10.1016/j.geoderma.2006.04.008>, 2006.
- 491 2. Anderson, T. M., Hopcraft, J. G. C., Eby, S., Ritchie, M., Grace, J. B., & Olf, H. Landscape-
492 scale analyses suggest both nutrient and antipredator advantages to Serengeti herbivore
493 hotspots. *Ecol.*, 91, 1519–1529, <https://doi.org/10.1890/09-0739.1>, 2010.
- 494 3. Aranibar, J. N., Macko, S. A., Anderson, I. C., Potgieter, A. L. F., Sowry, R. & Shugart, H.
495 H. Nutrient cycling responses to fire frequency in the Kruger National Park (South Africa) as
496 indicated by stable isotope analysis. *Isotopes Environ. Health Stud.*, 39, 141-158,
497 <https://doi.org/10.1080/1025601031000096736>, 2003.
- 498 4. Aria, Y. & Sparks, D. L. Phosphate reaction dynamics in soils and soil components: a
499 multiscale approach. *Adv. Agron.*, 94, 135-179, [https://doi.org/10.1016/S0065-](https://doi.org/10.1016/S0065-2113(06)94003-6)
500 [2113\(06\)94003-6](https://doi.org/10.1016/S0065-2113(06)94003-6), 2007.
- 501 5. Asner, G. P., Levick, S. R., Kennedy-Bowdoin, T., Knapp, D. E., Emerson, R., Jacobson, J.,
502 Colgan, M. S., & Martin, R. E. Large-scale impacts of herbivores on the structural diversity
503 of African savannas. *PNAS*, 106, 4947–4952, <https://doi.org/10.1073/pnas.0810637106>,
504 2009.

- 505 6. Augustine, D. J. Long-term, livestock-mediated redistribution of nitrogen and phosphorus in
506 an East African savanna. *J. Appl. Ecol.*, 40, 137-149, [https://doi.org/10.1046/j.1365-
2664.2003.00778.x](https://doi.org/10.1046/j.1365-
507 2664.2003.00778.x), 2003.
- 508 7. Barton, P. S., Cunningham, S. A., Lindenmayer, D. B., & Manning, A. D. The role of carrion
509 in maintaining biodiversity and ecological processes in terrestrial ecosystems. *Oecologia*,
510 171, 761–772, <https://doi.org/10.1007/s00442-012-2460-3>, 2013.
- 511 8. Barton, P.S. Carrion Ecology, Evolution, and Their Applications. Edited by: M.E. Benbow,
512 J.K. Tomberlin, A.M. Tarone. CRC Press, Boca Raton, FL, USA. 2016.
- 513 9. Barton, P. S., McIntyre, S., Evans, M. J., Bump, J. K., Cunningham, S. A., & Manning, A. D.
514 Substantial long-term effects of carcass addition on soil and plants in a grassy eucalypt
515 woodland. *Ecosphere*, 7, e01537, <https://doi.org/10.1002/ecs2.1537>, 2016.
- 516 10. Barton, P.S., Bump, J.K. Carrion decomposition. In: Carrion Ecology and Management.
517 Edited by: P.P. Olea, P. Mateo-Tomas, J.A. Sanchez-Zapata. Springer, NY, USA, 101-124,
518 2019.
- 519 11. Bates, D., Mächler, M., Bolker, B., & Walker, S. Fitting linear mixed-effects models using
520 lme4. *J. Stat. Softw.*, 67, 1–48, <https://doi.org/10.18637/jss.v067.i01>, 2015.
- 521 12. Britto, D. T., & Kronzucker, H. J. NH₄⁺ toxicity in higher plants: a critical review. *J. Plant*
522 *Physiol.*, 159, 567–584, <https://doi.org/10.1078/0176-1617-0774>, 2002.
- 523 13. Buitenwerf, R., Kulmatiski, A. & Higgins, S. I. Soil water retention curves for the major soil
524 types of the Kruger National Park. *Koedoe*, 56, a1228,
525 <http://dx.doi.org/10.4102/koedoe.v56i1.1228>, 2014.

- 526 14. Bump, J. K., Peterson, R. O., & Vucetich, J. A. Wolves modulate soil nutrient heterogeneity
527 and foliar nitrogen by configuring the distribution of ungulate carcasses. *Ecol.*, 90, 3159–
528 3167, <https://doi.org/10.1890/09-0292.1>, 2009.
- 529 15. Bump, J. K., Webster, C. R., Vucetich, J. A., Peterson, R. O., Shields, J. M., & Powers, M.
530 D. (2009). Ungulate carcasses perforate ecological filters and create biogeochemical hotspots
531 in forest herbaceous layers allowing trees a competitive advantage. *Ecosyst.*, 12, 996–1007,
532 <https://doi.org/10.1007/s10021-009-9274-0>, 2009.
- 533 16. Burnham, K. P. & Anderson, D. R. Model Selection and Multimodel Inference. Springer
534 New York, NY. <http://doi.org/10.1007/b97636>, 2002.
- 535 17. Campos-Arceiz, A., & Blake, S. Megagardeners of the forest – the role of elephants in seed
536 dispersal. *Acta Oecol.*, 37, 542–553, <https://doi.org/10.1016/j.actao.2011.01.014>, 2011.
- 537 18. Chen, J., Gutjahr, C., Bleckmann, A., & Dresselhaus, T. Calcium signaling during
538 reproduction and biotrophic fungal interactions in plants. *Mol. Plant*, 8, 595–611,
539 <https://doi.org/10.1016/j.molp.2015.01.023>, 2015.
- 540 19. Coe, M. The decomposition of elephant carcasses in the Tsavo (East) National Park, Kenya.
541 *J. Arid Environ.*, 1, 71–86, [https://doi.org/10.1016/S0140-1963\(18\)31756-7](https://doi.org/10.1016/S0140-1963(18)31756-7), 1978.
- 542 20. Coetsee, M. & Ferreira, S. Bridging science, management, and opinion: GLTFCA elephant
543 management [Conference presentation]. Savanna Science Network Meeting, Skukuza,
544 Kruger National Park, South Africa, 2023 March 5-9.
- 545 21. Coverdale, T. C., Kartzinel, T. R., Grabowski, K. L., Shriver, R. K., Hassan, A. A., Goheen,
546 J. R., Palmer, T. M., & Pringle, R. M. Elephants in the understory: opposing direct and
547 indirect effects of consumption and ecosystem engineering by megaherbivores. *Ecol.*, 97,
548 3219–3230, <https://doi.org/10.1002/ecy.1557>, 2016.

- 549 22. Craine, J. M., Morrow, C., & Stock, W. D. Nutrient concentration ratios and co-limitation in
550 South African grasslands. *New Phytol.*, 179, 829–836, [https://doi.org/10.1111/j.1469-](https://doi.org/10.1111/j.1469-8137.2008.02513.x)
551 [8137.2008.02513.x](https://doi.org/10.1111/j.1469-8137.2008.02513.x), 2008.
- 552 23. Croghan C. & Egeghy P. P., Methods of dealing with values below the limit of detection
553 using SAS. *Southern SAS User Group*, 22, 2003.
- 554 24. Danell, K., Berteaux, D., & Bråthen, K. A. Effect of muskox carcasses on nitrogen
555 concentration in tundra vegetation. *Arctic*, 55, 389–392, <http://www.jstor.org/stable/40512497>,
556 2002.
- 557 25. Davies, A. B., Levick, S. R., Robertson, M. P., van Rensburg, B. J., Asner, G. P. & Parr, C.
558 L. Termite mounds differ in their importance for herbivores across savanna types, seasons
559 and spatial scales. *Oikos*, 125, 726-734, <https://doi.org/10.1111/oik.02742>, 2016.
- 560 26. Doughty, C. E., Roman, J., Faurby, S., Wolf, A., Haque, A., Bakker, E. S., Malhi, Y.,
561 Dunning, J. B., Jr, & Svenning, J.-C. Global nutrient transport in a world of giants. *PNAS*,
562 113, 868–873, <https://doi.org/10.1073/pnas.1502549112>, 2016.
- 563 27. Doughty, C. E., Wolf, A., & Malhi, Y. The legacy of the Pleistocene megafauna extinctions
564 on nutrient availability in Amazonia. *Nat. Geosci.*, 6, 761–764,
565 <https://doi.org/10.1038/ngeo1895>, 2013.
- 566 28. Esala, M. J. Changes in the extractable ammonium- and nitrate-nitrogen contents of soil
567 samples during freezing and thawing. *Commun. Soil Sci. Plant Anal.*, 26, 61-68,
568 <https://doi.org/10.1080/00103629509369280>, 1995.
- 569 29. Flannery, T. F. Pleistocene faunal loss: implications of the aftershock for Australia's past and
570 future. *Archaeol. Ocean.*, 25, 45–55, <https://doi.org/10.1002/j.1834-4453.1990.tb00232.x>,
571 1990.

- 572 30. Gertenbach, W. Landscapes of the Kruger National Park. *Koedoe*, 26, 9-121,
573 <https://doi.org/10.4102/koedoe.v26i1.591>, 1983.
- 574 31. Goldenberg, S. Z. & Wittemyer, G. Elephant behavior toward the dead: A review and
575 insights from field observations. *Primates*, 61, 119-128, [https://doi.org/10.1007/s10329-019-](https://doi.org/10.1007/s10329-019-00766-5)
576 [00766-5](https://doi.org/10.1007/s10329-019-00766-5), 2020.
- 577 32. Grant, C. C., & Scholes, M. C. The importance of nutrient hot-spots in the conservation and
578 management of large wild mammalian herbivores in semi-arid savannas. *Biol. Conserv.*, 130,
579 426–437, <https://doi.org/10.1016/j.biocon.2006.01.004>, 2006.
- 580 33. Gray, E. F. & Bond, W. Soil nutrients in an African forest/savanna mosaic: Drivers or
581 driven? *S. Afr. J. Bot.*, 101, 66-72, <https://doi.org/10.1016/j.sajb.2015.06.003>, 2015.
- 582 34. Guy, T. J., Hutchinson, M. C., Baldock, K. C. R., Kayser, E., Baiser, B., Staniczenko, P. P.
583 A., Goheen, J. R., Pringle, R. M., & Palmer, T. M. Large herbivores transform plant-
584 pollinator networks in an African savanna. *Curr. Biol.*, 2964–2971,
585 <https://doi.org/10.1016/j.cub.2021.04.051>, 2021.
- 586 35. Hocking, M. D. & Reynolds, J. D. Nitrogen uptake by plants subsidized by Pacific salmon
587 carcasses: a hierarchical experiment. *Can. J. For. Res.*, 42, 908-917,
588 <https://doi.org/10.1139/x2012-045>, 2012.
- 589 36. Holdo, R. M. Effects of fire history and N and P fertilization on seedling biomass, specific
590 leaf area, and root:shoot ratios in a South African savannah. *S. Afr. J. Bot.*, 86, 5–8,
591 <https://doi.org/10.1016/j.sajb.2013.01.005>, 2013.
- 592 37. Holdo, R. M. & Mack, M. C. Functional attributes of savanna soils: contrasting effects of
593 tree canopies and herbivores on bulk density, nutrients and moisture dynamics. *J. Ecol.*, 102,
594 1171-1182, <https://doi.org/10.1111/1365-2745.12290>, 2014.

- 595 38. Hu, L., Wu, Z., Robert, C. A. M., Ouyang, X., Züst, T., Mestrot, A., Xu, J., & Erb, M. Soil
596 chemistry determines whether defensive plant secondary metabolites promote or suppress
597 herbivore growth. *PNAS*, 118, e2109602118, <https://doi.org/10.1073/pnas.2109602118>,
598 2021.
- 599 39. Jobbágy, E. G., & Jackson, R. B. The uplift of soil nutrients by plants: biogeochemical
600 consequences across scales. *Ecol.*, 85, 2380–2389, <https://doi.org/10.1890/03-0245>, 2004.
- 601 40. Joern, A., Provin, T., & Behmer, S. T. Not just the usual suspects: insect herbivore
602 populations and communities are associated with multiple plant nutrients. *Ecol.*, 93, 1002–
603 1015, <https://doi.org/10.1890/11-1142.1>, 2012.
- 604 41. Kaspari, M. The invisible hand of the periodic table: how micronutrients shape ecology.
605 *Annu. Rev. Ecol. Evol. Syst.*, 52, 199–219, [https://doi.org/10.1146/annurev-ecolsys-012021-
606 090118](https://doi.org/10.1146/annurev-ecolsys-012021-090118), 2021.
- 607 42. Keenan, S. W., Schaeffer, S. M., Jin, V. L. & DeBruyn, J. M. Mortality hotspots: nitrogen
608 cycling in forest soils during vertebrate decomposition. *Soil Biol. Biochem.*, 121, 165-176,
609 <https://doi.org/10.1016/j.soilbio.2018.03.005>, 2018.
- 610 43. Keenan, S. W., Schaeffer, S. M., and DeBruyn, J. M. Spatial changes in soil stable isotopic
611 composition in response to carrion decomposition, *Biogeosciences*, 16, 3929–3939,
612 <https://doi.org/10.5194/bg-16-3929-2019>, 2019.
- 613 44. Keenan, S. W., & Beeler, S. R. Long-term effects of buried vertebrate carcasses on soil
614 biogeochemistry in the Northern Great Plains. *PloS One*, 18, e0292994,
615 <https://doi.org/10.1371/journal.pone.0292994>, 2023.

- 616 45. Khomo, L., Trumbore, S., Bern, C. R. & Chadwick, O. A. Timescales of carbon turnover in
617 soils with mixed crystalline mineralogies. *SOIL*, 3, 17-30, [https://doi.org/10.5194/soil-3-17-](https://doi.org/10.5194/soil-3-17-2017)
618 [2017](https://doi.org/10.5194/soil-3-17-2017), 2017.
- 619 46. Lathwell, D. J. & Grove, T. L. Soil-plant relationships in the tropics. *Annu. Rev. Ecol. Syst.*,
620 17, 1-16, <https://www.jstor.org/stable/2096986>, 1986.
- 621 47. Lemoine, N. P., Budny, M. L., Rose, E., Lucas, J., & Marshall, C. W. Seasonal soil moisture
622 thresholds inhibit bacterial activity and decomposition during drought in a tallgrass prairie.
623 *Oikos*, 2024, e10210, <https://doi.org/10.1111/oik.10201>, 2023.
- 624 48. Macdonald, B. C. T., Farrell, M., Tuomi, S., Barton, P. S., Cunningham, S. A., & Manning,
625 A. D. Carrion decomposition causes large and lasting effects on soil amino acid and peptide
626 flux. *Soil Biol. Biochem.*, 69, 132–140, <https://doi.org/10.1016/j.soilbio.2013.10.042>, 2014.
- 627 49. Moleón, M., Sánchez-Sapata, J. A., Sebastián-González, E. & Owen-Smith, N. Carcass size
628 shapes the structure and functioning of an African scavenging assemblage. *Oikos*, 124, 1391-
629 1403, <https://doi.org/10.1111/oik.02222>, 2015.
- 630 50. Monk, J. D., Donadio, E., Smith, J. A., Perrig, P. L., Middleton, A. D., & Schmitz, O. J.
631 Predation and biophysical context control long-term carcass nutrient inputs in an Andean
632 ecosystem. *Ecosyst.*, 27, 346–359, <https://doi.org/10.1007/s10021-023-00893-7>, 2024.
- 633 51. Morris, A. W., Smith, I., Chakrabarti, S., Lala, F., Nyaga, S. & Bump, J. K. Eating an
634 elephant, one bite at a time: predator interactions at carrion bonanzas. *Food Webs*, 37,
635 e00304, <https://doi.org/10.1016/j.fooweb.2023.e00304>, 2023.
- 636 52. Mphepya, J. N., Galy-Lacaux, C., Lacaux, J. P., Held, G., & Pienaar, J. J. Precipitation
637 chemistry and wet deposition in Kruger National Park, South Africa. *J. Atmos. Chem.*, 53,
638 169–183, <https://doi.org/10.1007/s10874-005-9005-7>, 2006.

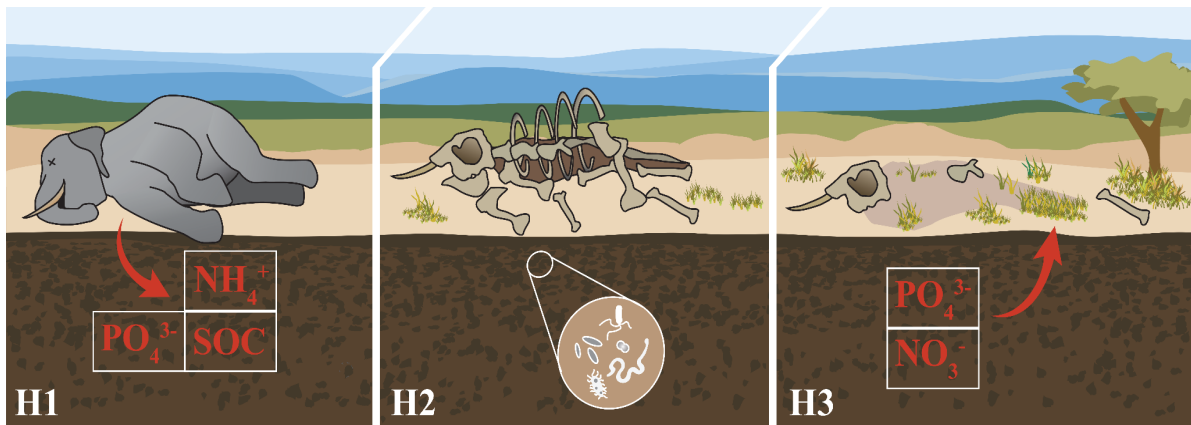
- 639 53. Oksanen J, Simpson G, Blanchet F, Kindt R, Legendre P, Minchin P, O'Hara R, Solymos P,
640 Stevens M, Szoecs E, Wagner H, Barbour M, Bedward M, Bolker B, Borcard D, Carvalho G,
641 Chirico M, De Caceres M, Durand S, Evangelista H, FitzJohn R, Friendly M, Furneaux B,
642 Hannigan G, Hill M, Lahti L, McGlinn D, Ouellette M, Ribeiro Cunha E, Smith T, Stier A,
643 Ter Braak C, Weedon J. Community Ecology Package. R package version 2.6-4,
644 <https://CRAN.R-project.org/package=vegan>, 2022.
- 645 54. Olea, P.P, Mateo-Tomas, P., Sanchez-Zapata, J.A. (eds.) Carrion Ecology and Management.
646 Springer, NY, USA, 2019.
- 647 55. Owen-Smith, N. Megafaunal extinctions: the conservation message from 11,000 years B.P.
648 *Conserv. Biol.*, 3, 405–412, <https://www.jstor.org/stable/2386221>, 1989.
- 649 56. Owen-Smith, N., & Mills, M. G. L. Predator-prey size relationships in an African large-
650 mammal food web. *J. Anim. Ecol.*, 77, 173–183, [https://doi.org/10.1111/j.1365-](https://doi.org/10.1111/j.1365-2656.2007.01314.x)
651 [2656.2007.01314.x](https://doi.org/10.1111/j.1365-2656.2007.01314.x), 2008.
- 652 57. Pandey, N. Role of micronutrients in reproductive physiology of plants. *Plant Stress*, 4, 1-13.
653 <https://www.semanticscholar.org/paper/af9a8662b83613f6e0d5e538ed33f3add4a1d5a1>,
654 2010.
- 655 58. Parmenter, R. R., & MacMahon, J. A. Carrion decomposition and nutrient cycling in a
656 semiarid shrub–steppe ecosystem. *Ecol. Monogr.*, 79, 637–661, [https://doi.org/10.1890/08-](https://doi.org/10.1890/08-0972.1)
657 [0972.1](https://doi.org/10.1890/08-0972.1), 2009.
- 658 59. Pellegrini, A. F. A. Nutrient limitation in tropical savannas across multiple scales and
659 mechanisms. *Ecol.*, 97, 313–324, <https://doi.org/10.1890/15-0869.1>, 2016.
- 660 60. Prosser, J. I. Soil Nitrifiers and Nitrification. In Nitrification. ASM Press, pp. 347-383, 2014.

- 661 61. Quaggiotto, M.-M., Evans, M. J., Higgins, A., Strong, C., & Barton, P. S. Dynamic soil
662 nutrient and moisture changes under decomposing vertebrate carcasses. *Biogeochemistry*,
663 146, 71–82, <https://doi.org/10.1007/s10533-019-00611-3>, 2019.
- 664 62. R Core Team. R: A language and environment for statistical computing. R Foundation for
665 Statistical Computing, Vienna, Austria. <https://www.R-project.org/>, 2022.
- 666 63. Ries, L. P., & Shugart, H. H. Nutrient limitations on understory grass productivity and
667 carbon assimilation in an African woodland savanna. *J. Arid Environ.*, 72, 1423–1430,
668 <https://doi.org/10.1016/j.jaridenv.2008.02.013>, 2008.
- 669 64. Ripple, W. J., Newsome, T. M., Wolf, C., Dirzo, R., Everatt, K. T., Galetti, M., Hayward, M.
670 W., Kerley, G. I. H., Levi, T., Lindsey, P. A., Macdonald, D. W., Malhi, Y., Painter, L. E.,
671 Sandom, C. J., Terborgh, J., & Van Valkenburgh, B. Collapse of the world’s largest
672 herbivores. *Sci. Adv.*, 1, e1400103, <https://doi.org/10.1126/sciadv.1400103>, 2015.
- 673 65. Risch, A. C., Frossard, A., Schütz, M., Frey, B., Morris, A. W., & Bump, J. K. Effects of elk
674 and bison carcasses on soil microbial communities and ecosystem functions in Yellowstone,
675 USA. *Funct. Ecol.*, 34, 1933–1944, <https://doi.org/10.1111/1365-2435.13611>, 2020.
- 676 66. Roman, J., Estes, J. A., Morissette, L., Smith, C., Costa, D., McCarthy, J., Nation, J. B.,
677 Nicol, S., Pershing, A., & Smetacek, V. *Whales as marine ecosystem engineers. Front. Ecol.*
678 *Environ.*, 12, 377–385, <https://doi.org/10.1890/130220>, 2014.
- 679 67. Rughöft, S., Hermann, M., Lazar, C. S., Cesarz, S., Levick, S. R., Trumbore, S. E. & Küsel,
680 K. Community composition and abundance of bacterial, archaeal and nitrifying populations
681 in savanna soils on contrasting bedrock material in Kruger National Park, South Africa.
682 *Front. Microbiol.*, 7, <https://doi.org/10.3389/fmicb.2016.01638>, 2016.

- 683 68. Sardans, J., & Peñuelas, J. Potassium control of plant functions: ecological and agricultural
684 implications. *Plants*, 10, <https://doi.org/10.3390/plants10020419>, 2021.
- 685 69. Schmitz, O. J., Wilmers, C. C., Leroux, S. J., Doughty, C. E., Atwood, T. B., Galetti, M.,
686 Davies, A. B., & Goetz, S. J. Animals and the zoogeochemistry of the carbon cycle. *Science*,
687 362, <https://doi.org/10.1126/science.aar3213>, 2018.
- 688 70. Skarpe, C., Aarrestad, P. A., Andreassen, H. P., Dhillion, S. S., Dimakatso, T., du Toit, J. T.,
689 Duncan, Halley, J., Hytteborn, H., Makhabu, S., Mari, M., Marokane, W., Masunga, G.,
690 Ditshoswane, M., Moe, S. R., Mojaphoko, R., Mosugelo, D., Motsumi, S., Neo-Mahupeleng,
691 G., ... Wegge, P. The return of the giants: ecological effects of an increasing elephant
692 population. *Ambio*, 33, 276–282, <http://www.jstor.org/stable/4315497>, 2004.
- 693 71. Sollen-Norrin, M. & Rintoul-Hynes, N. L. J. Soil sample storage conditions affect
694 measurements of pH, potassium, and nitrogen. *SSSAJ*, 88, 930-941,
695 <https://doi.org/10.1002/saj2.20653>, 2024.
- 696 72. Sterner, R. W., & Elser, J. J. Ecological Stoichiometry: The Biology of Elements from
697 Molecules to the Biosphere. Princeton University Press.
698 <http://www.jstor.org/stable/j.ctt1jktrp3>, 2002.
- 699 73. Subalusky, A. L., Dutton, C. L., Rosi, E. J., & Post, D. M. Annual mass drownings of the
700 Serengeti wildebeest migration influence nutrient cycling and storage in the Mara River.
701 *PNAS*, 114, 7647–7652, <https://doi.org/10.1073/pnas.1614778114>, 2017.
- 702 74. Subalusky, A.L., Dutton, C.L., Rosi, E.J, Puth, L.M., Post, D.M. River of bones: wildebeest
703 skeletons leave a legacy of mass mortality in Mara River, Kenya. *Front. Ecol. Evol.*, 8,
704 <https://doi.org/10.3389/fevo.2020.00031>, 2020.

- 705 75. Towne, E. G. Prairie vegetation and soil nutrient responses to ungulate carcasses. *Oecologia*,
706 122, 232–239, <https://www.jstor.org/stable/4222536>, 2000.
- 707 76. Turner, B. L. & Romero, T. E. Short-term changes in extractable inorganic nutrients during
708 storage of tropical rainforest soils. *SSSAJ*, 73, 1972-1979,
709 <https://doi.org/10.2136/sssaj2008.0407>, 2009.
- 710 77. Turner, W. C., Kausrud, K. L., Krishnappa, Y. S., Cromsigt, J. P. G. M., Ganz, H. H.,
711 Mapaure, I., Cloete, C. C., Havarua, Z., Küsters, M., Getz, W. M., & Stenseth, N. C. Fatal
712 attraction: vegetation responses to nutrient inputs attract herbivores to infectious anthrax
713 carcass sites. *Proc. R. Soc. B*, 281, <https://doi.org/10.1098/rspb.2014.1785>, 2014.
- 714 78. van Klink, R., van Laar-Wiersma, J., Vorst, O., & Smit, C. Rewilding with large herbivores:
715 Positive direct and delayed effects of carrion on plant and arthropod communities. *PloS One*,
716 15, e0226946, <https://doi.org/10.1371/journal.pone.0226946>, 2020.
- 717 79. Venter, F. J., Scholes, R. J. & Eckhardt, H. C. Abiotic template and its associated vegetation
718 pattern. In: J. T. Du Toit, K. H. Rogers, H. C. Biggs, eds. *The Kruger experience: ecology*
719 *and management of savanna heterogeneity*. Washington, DC, USA: Island Press, 83–129,
720 2003.
- 721 80. Wiersum, L. K. Uptake of nitrogen and phosphorus in relation to soil structure and nutrient
722 mobility. *Plant Soil*, 16, 62–70, <https://doi.org/10.1007/BF01378158>, 1962.
- 723 81. Wigley, B. J., Coetsee, C., Fritz, C. & Bond, W. J. Herbivores shape woody plant
724 communities in the Kruger National Park: lessons from three long-term exclosures: original
725 research. *Koedoe*, 56, <http://dx.doi.org/10.4102/koedoe.v56i1.1165>, 2014.
- 726 82. Yang, L. H. Periodical cicadas as resource pulses in North American forests. *Science*, 306,
727 1565–1567, <https://doi.org/10.1126/science.1103114>, 2004.

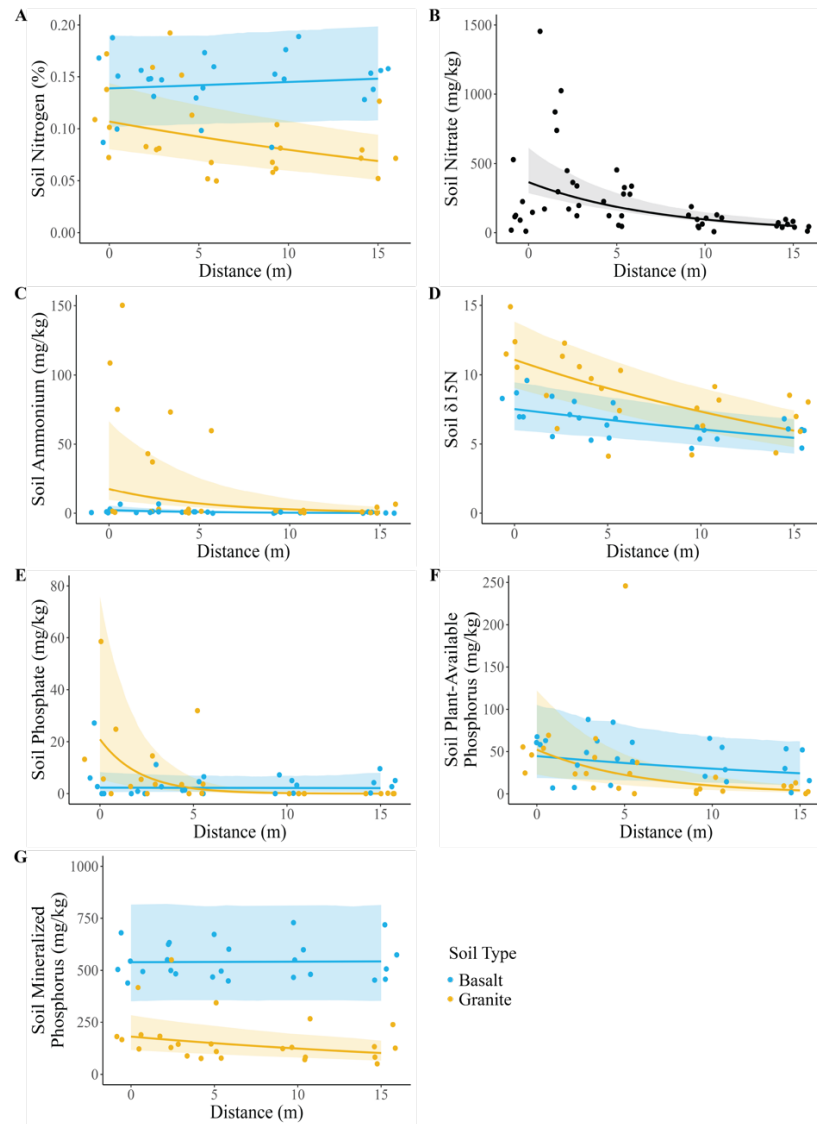
- 728 83. Yang, L. H. Pulses of dead periodical cicadas increase herbivory of American bellflowers.
729 *Ecol.*, 89, 1497–1502, <https://doi.org/10.1890/07-1853.1>, 2008.
- 730 84. Yong, S. K., Jalaludin, N. H., Brau, E., Shamsudin, N. N., & Heo, C. C. Changes in soil
731 nutrients (ammonia, phosphate and nitrate) associated with rat carcass decomposition under
732 tropical climatic conditions. *Soil Res.*, 57, 482–488, <https://doi.org/10.1071/SR18279>, 2019.



733

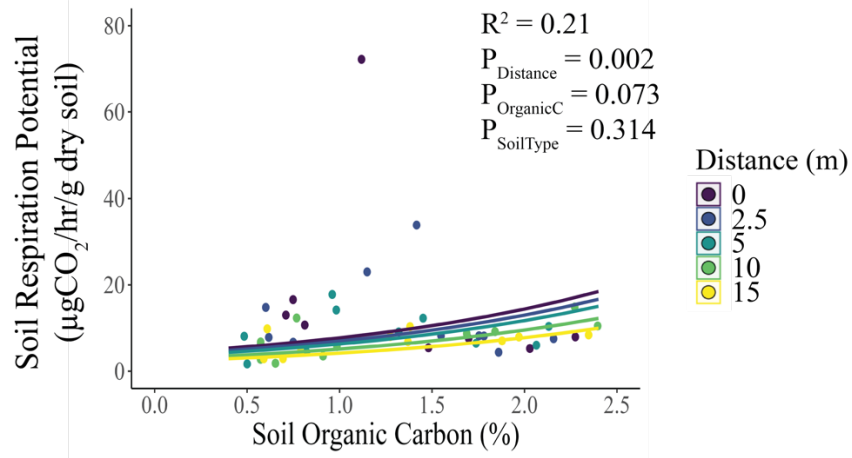
734 **Figure 1.** Hypothesized impacts of elephant megacarcasses on soil and plant nutrients. First
 735 (H1), we hypothesized that elephant carcasses would release pulses of nutrients into the soil,
 736 resulting in higher concentrations of soil ions such as nitrogen (ammonium, $[\text{NH}_4]^+$), phosphorus
 737 (phosphate, $[\text{PO}_4]^{3-}$), and soil organic C. Second (H2), we hypothesized that C inputs from the
 738 carcass would result in increased soil microbial respiration potential. Third (H3), we
 739 hypothesized that plants would take up nutrients from the carcass soil, resulting in plants with
 740 distinct nutrient profiles and increased concentrations of key limiting nutrients such as N and P.

741 Image credit: Kirsten Boeh.



742

743 **Figure 2.** Soil N and P responses to elephant carcasses. (A) Soil N (%) was greater in basaltic
 744 soils, and in granitic soils it decreased with distance from the carcass site. (B) Soil nitrate
 745 nitrogen decreased with distance but did not differ with soil type. (C) Soil ammonium nitrogen
 746 and (D) $\delta^{15}\text{N}$ were both greater in granitic soils and decreased with distance from the carcass. (E)
 747 Soil phosphate, (F) plant-available P, and (G) mineralized P decreased with distance in granitic
 748 soils but not basaltic soils. Points represent individual measurements taken at 0, 2.5, 5, 10, and
 749 15m and are offset to be visible when they would otherwise overlap. Lines show predictions
 750 calculated from the top model (see Table S1). Shading indicates the 95% confidence interval.



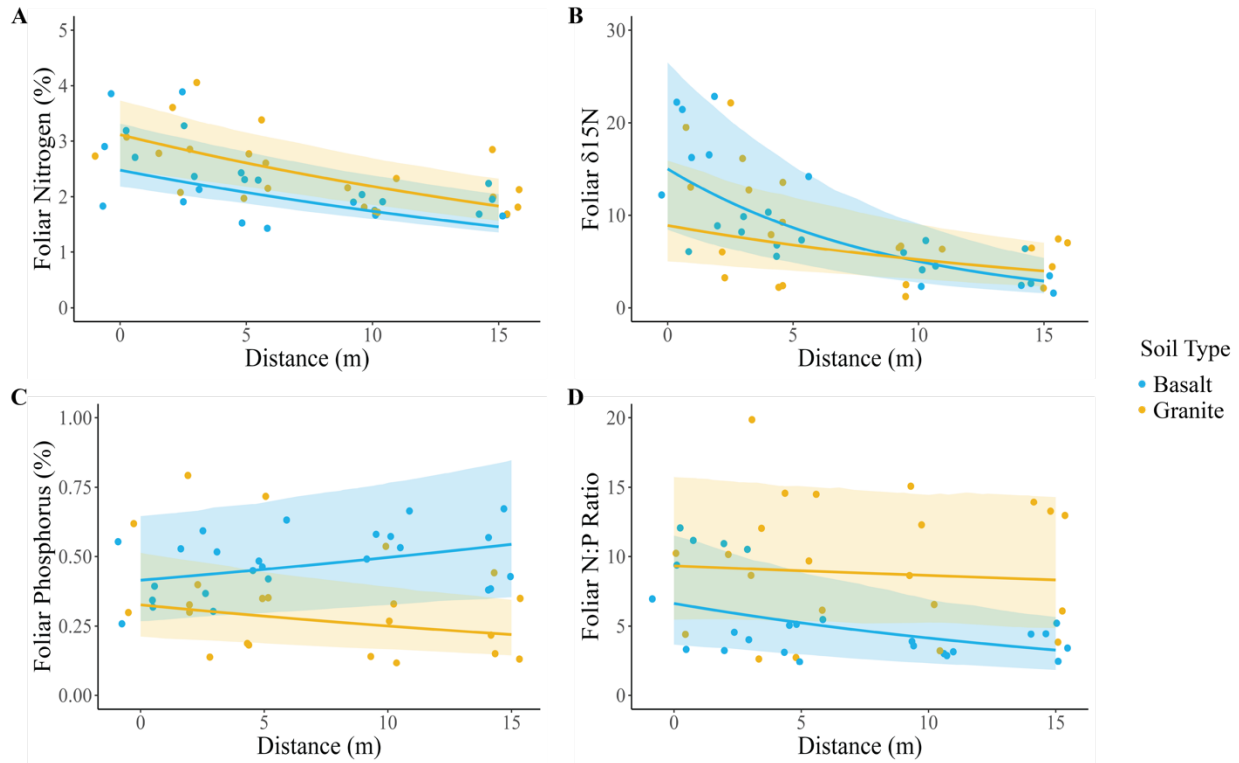
751

752 **Figure 3.** Soil respiration potential was marginally positively correlated with soil organic C (%)

753 and decreased significantly with distance from the carcass. Points represent individual

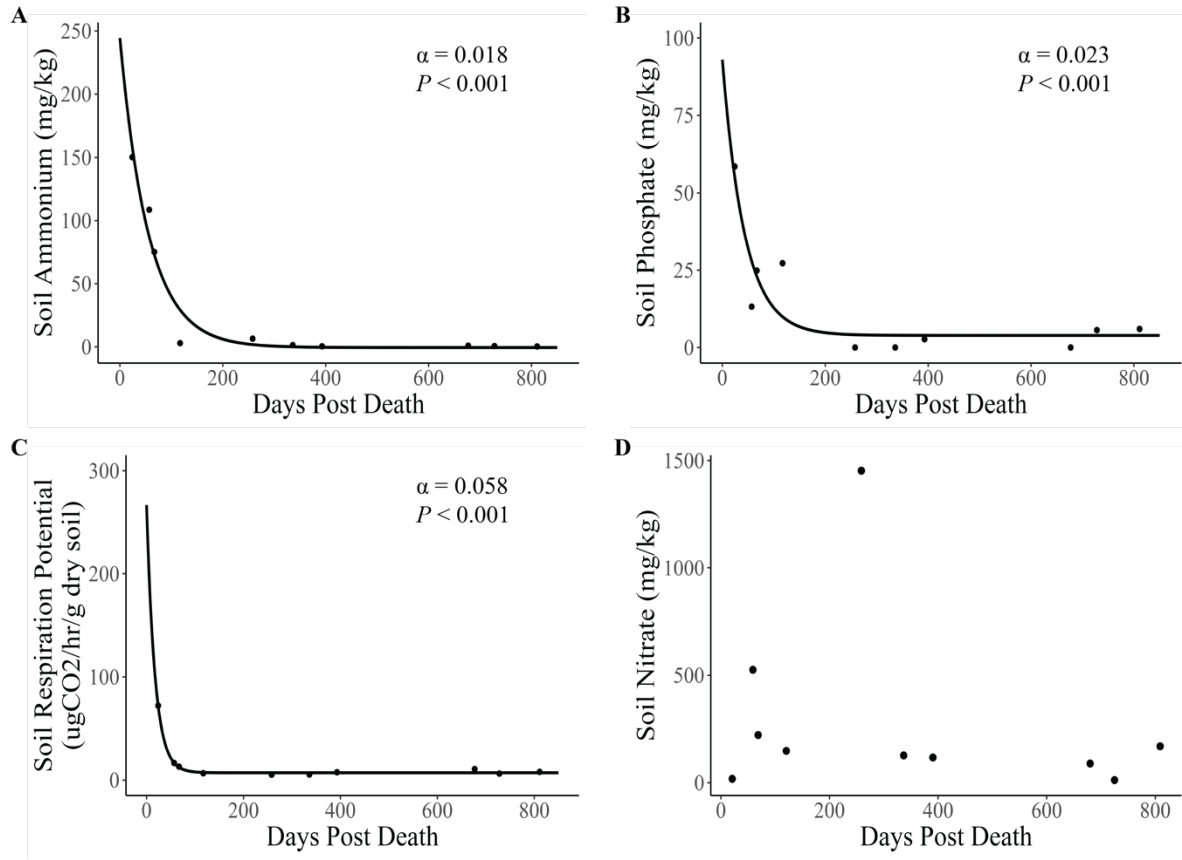
754 measurements taken at 0, 2.5, 5, 10, and 15m and are offset to be visible when they would

755 otherwise overlap. Lines represent model predictions.



756

757 **Figure 4.** Foliar N and P responses to elephant carcasses. (A) Foliar %N and (B) $\delta^{15}\text{N}$ both
 758 decreased with distance from the carcass center. (C) Foliar P was greater in basaltic soils and
 759 decreased with distance in granitic soils. (D) Foliar N:P ratio was greater in granitic soils and
 760 decreased with distance from the carcass center. Points represent individual measurements taken
 761 at 0, 2.5, 5, 10, and 15m and are offset to be visible when they would otherwise overlap. Lines
 762 show predictions calculated from the top model (see Table S2). Shading indicates the 95%
 763 confidence interval. Three of the ten sites had bare ground at the 0 m distance, resulting in a
 764 sample size of 7 sites for that distance and 10 for the other distances.



765

766 **Figure 5.** Relationship between carcass age and key soil metrics (soil ion concentrations and
 767 respiration potential). Lines represent predictions from exponential decay models, with α equal
 768 to the rate of decay. (A) Soil ammonium, (B) phosphate, and (C) respiration potential all
 769 decreased significantly with carcass age. The model for (D) soil nitrate failed to converge. Points
 770 represent individual measurements taken at the center of the carcass site (distance = 0.5m).